

Marta Hałas-Wiśniewska, Magdalena Izdebska, Wioletta Zielińska, Joanna Kralska, Patryk Zawadka, Alina Grzanka

Department of Histology and Embryology, Nicolas Copernicus University in Torun, Faculty of Medicine, Collegium Medicum in Bydgoszcz, Poland

The effect of sanguinarine on the RPMI-7951 and A375 melanoma cell lines

Corresponding author:

Marta Hałas-Wiśniewska, Department of Histology and Embryology, Nicolas Copernicus University in Torun, Faculty of Medicine, Collegium Medicum in Bydgoszcz, Karłowicza 24 Str., 85-092 Bydgoszcz, Poland; e-mail: mhalas@cm.umk.pl

ABSTRACT

Background: Considering the resistance of melanoma to standard treatment protocols, the possibility of metastasis and the high mortality risk, the selection of new alternatives seems to be necessary. Compounds of natural origin are a promising option in anti-cancer therapy. One of them — sanguinarine has a wide spectrum of pro-health properties. Thus, the study aimed to assess the effect of the alkaloid on selected melanoma cellular models.

Material and methods: Two types of melanoma cell lines were used in the study — A375 and RPMI-7951. The cells were treated with sanguinarine at concentrations ranging from 0.1 to 2 μ M for 24 and 48 h. The influence of the alkaloid on such processes as cell death, cell cycle, organization of the main cytoskeletal proteins and migration potential was assessed. In addition, the sensitivity of selected cell lines to sanguinarine was evaluated based on the MTT assay.

Results: The results showed that sanguinarine caused a dose-dependent decrease in cell survival compared to the untreated control. Further studies confirmed that it resulted from the pro-apoptotic and anti-proliferative action of the alkaloid. There were also significant changes in the organization of cytoskeletal proteins and the number of cells visible after fluorescent labelling. Moreover, in A375 cells, characteristics of entosis and mitotic catastrophe were noted. Sanguinarine-induced impaired cell migration was also confirmed.

Conclusion: According to the authors' knowledge, they are the first to present the influence of sanguinarine on the basic life processes of the RPMI-7951 cell line and supplement the knowledge regarding the A375 melanoma cells. The present results confirm the anticancer properties of the alkaloid (cytotoxicity, anti-migratory and pro-apoptotic effect).

Key words: sanguinarine, melanoma, A375, RPMI-7951

Medical Research Journal 2023;
10.5603/MRJ.a2023.0008
Copyright © 2023 Via Medica
ISSN 2451-2591
e-ISSN 2451-4101

Introduction

Nowadays, cancers are one of the leading causes of death, second only to cardiovascular diseases. The rise in their occurrence is a severe diagnostic problem. Melanomas — malignant cancers originating from melanocytes are the most rapidly increasing malignancy in the population, which follow lung cancer in mortality rate. Early recognition and excision of affected tissue are key to positive outcomes [1]. Out of many different Melanoma subtypes, three are considered the most common: Superficial Spreading Melanoma (SSM, the most common type), Nodular Melanoma (NM), and Lentigo Maligna Melanoma (LMM) [2, 3]. Melanomas in the vertical growth phase show metastatic capability, which makes them more difficult to cure once the process has

begun. If surgery cannot be performed, for example, in metastatic disease, radiotherapy, phototherapy, or chemotherapy can be applied [1, 3]. The effect of these therapies might vary as they can impair quality of life and further recovery. Thus, alternative therapies are sought. One of the possibilities is the use of alkaloids, for example, sanguinarine [4, 5].

Alkaloids are plant metabolites used both in natural medicine as well as in conventional therapies. Apart from their widely known uses as antibacterial, antifungal, or anti-inflammatory agents, they are tested for their anticancer properties as they target multiple signalling pathways and influence the ability of cancer cells to proliferate and differentiate [6, 7]. Studies show that alkaloids are effective against many types of cancers, for example, lung, colon, breast, and skin [5].

Sanguinarine (SAN) is a benzo phenanthridine alkaloid found in multiple herbs, most commonly in *Sanguinaria Canadensis*. As with many alkaloids, it also exhibits antioxidant, anti-inflammatory, proapoptotic, and antiproliferative activities in many types of cancer, as shown in both *in vitro* and *in vivo* studies [5, 7]. For example, studies on non-small cell lung cancer have shown that SAN caused growth inhibition, reduced colony-forming abilities, and increased apoptotic cell population [7, 8]. Moreover, the use of the alkaloid in melanoma has been widely studied in recent years. Its antineoplastic potential makes it an attractive alternative to conventional therapy, which may lack efficiency [4, 5]. Sanguinarine is toxic to most cells, which may be due to DNA intercalation, inhibition of ion pumps and interaction with cytoskeletal components. At higher doses or in direct contact with skin it can cause tissue necrosis, but used at low doses, SAN exhibits specificity to cancer cells [9, 10].

The study aimed to determine the effectiveness and optimal concentration of sanguinarine on the A375 and RPMI-7951 melanoma cell lines. To the authors' knowledge, they are the first to show the impact of SAN on the RPMI-7951 cell line.

Material and methods

Cell culture, treatment and MTT assay

The research material was two human melanoma cell lines (A375 and RPMI-7951) obtained from ATCC (American Type Culture Collection). The cells were cultured as monolayers using DMEM (Dulbecco's Modified Eagle Medium, Lonza) and EMEM (Eagle's Minimum Essential Medium, Lonza), respectively. The culture media were supplemented with 10% foetal bovine serum (FBS, Sigma Aldrich) and antibiotics (penicillin/streptomycin, Sigma-Aldrich). The cell culture was carried out in an incubator under optimal growth conditions: constant humidity of 95%, a temperature of 37°C, and an air atmosphere with 5% CO₂ concentration. A375 and RPMI-7951 cells were treated with SAN in doses: 0.1, 0.5, 1, 1.5, and 2 μ M. 24 and 48 h after treatment, an MTT cytotoxicity assay was performed. Based on the results, three alkaloid concentrations were selected for further analysis - 0.1, 0.5, and 1 μ M. The cells were incubated with the compound for 24 and 48 h. The control consisted of cells grown under identical conditions without sanguinarine.

Cell death and cell cycle analysis

A375 and RPMI-7951 cells grown in 12-well plates were detached using trypsin. To analyse cell death the cell pellet was resuspended in 100 μ l ABB (Annexin-binding buffer) supplemented with 5 μ l AV (Annexin

V) and 1 μ l PI (propidium iodide) and incubated in the dark for 20 min at room temperature (Life Technologies; Thermo Fisher Scientific, Inc). In turn, for cell cycle analysis the cells were fixed in Cytofix/Cytoperm Fixation Permeabilization Solution (30 min, RT, BD Biosciences), washed with Perm/Wash Buffer (BD Biosciences) and centrifuged (5 minutes, 300 x g). After discarding the supernatant, the cell pellet was resuspended in 80% ice-cold ethanol and placed at -20°C for a minimum of 24 h. The samples were centrifuged, and the supernatant was removed. After washing with PBS, the cell pellet was resuspended in 200 μ l FxCycle™ PI/RNase Staining Solution (BD Biosciences) and incubated for 30 minutes in the dark. In both methods, the last step was analysis in a flow cytometer (Guava EasyCyte 6HT-2L Cytometer (Merck KGaA) and FlowJo software (version 10.07; FlowJo LLC).

Organization of main cytoskeleton proteins

Actin filaments and vimentin were labelled in the control and SAN-treated cells (0.1, 0.5, and 1 μ M) with different exposure times: 24 h and 48 h. In the first step, cells were fixed in 4% paraformaldehyde for 20 minutes and washed with PBS (3x 5 min, RT). The next step was the permeabilization of the cell membrane using a 0.25% Triton X-100 solution. The cells were incubated for 20 minutes in a 4% BSA solution (Sigma-Aldrich) to block the background and eliminate non-specific antibody binding. After this time, the mouse primary anti-vimentin antibody (Invitrogen) was applied at a 1:100 dilution and incubated for one hour. After washing with PBS (3x 5 min, RT), the research material was incubated for an hour with the anti-mouse secondary antibody conjugated with Alexa Fluor 594 (Invitrogen). F-actin was stained with phalloidin conjugated to Alexa Fluor 488 (Invitrogen) at a dilution of 1:40 (20 min). To visualize cell nuclei, cells were stained with DAPI (Sigma-Aldrich) for 10 minutes and washed with PBS (3x 5 min, RT). In the last stage, slides with preparations were sealed in Aqua-Poly/Mount medium (Polysciences) and analysed using a laser scanning confocal microscope C1 (Nikon) with an immersion objective and a magnification of 60x. The Nikon EZ-C1 3.80 program was used for computer image analysis.

Analysis of transwell migration assay

To assess migratory abilities, control and SAN-treated cells (24 h and 48 h) were detached with trypsin and seeded at a density of 100 000/transwell for another day on inserts with 0.8 μ m pores in medium with 1% FBS (upper compartment) placed in a 24-well plate in medium supplemented with 15% FBS (lower compartment). Next, the cells were fixed using 4% paraformaldehyde and 80% methanol. The cells from the lower chamber

were labelled with 0.4% crystal violet, while cells that did not migrate to the other side of the membrane were removed (upper chamber). The inserts were photographed using an Eclipse E800 microscope (Nikon) equipped with a DS-5Mc-U1 CCD camera (Nikon) and an image analysis system NIS-Elements (version 3.30; Nikon). Cells were counted and their number was compared to the control group.

Statistical analysis of data

Statistical analysis of the obtained results was carried out using two tests: the non-parametric Wilcoxon test of two groups of variables (MTT assay) and non-parametric 2way ANOVA with Dunnett's multiple comparisons tests (cell cycle), Kruskal–Wallis with Dunn's post hoc test (cell death and transwell migration assay). The level of significance was $p < 0.05$, and statistically significant differences are marked with "*". GraphPadPrism 8.01 (GraphPad Software) was used to perform the analyses.

Results

Assessment of cytotoxicity – MTT assay

The effect of sanguinarine on the survival of human melanoma cells of the A375 and RPMI-7951 lines was assessed using the MTT test after 24 and 48 hours of ex-

posure. Five concentrations of sanguinarine were used in the experiments: 0.1, 0.5, 1, 1.5, and 2 μM . The alkaloid used in the study showed a dose-dependent effect on the survival and proliferation of the cells. Statistically significant differences were observed compared to the control for all doses ($p < 0.05$; Fig. 1A-D). The results indicate that the RPMI-7951 cell line is more sensitive to the selected alkaloid for both incubation times (Fig. 1C, D). Three concentrations were selected for further research - 0.1, 0.5, and 1 μM , and two incubation times: 24 h and 48 h (Fig. 1).

Cell death and cell cycle analysis

Flow cytometry was applied to assess cell death and changes in the distribution of cell cycle phases. In the case of A375 cells, a statistically significant decrease in the percentage of viable cells was demonstrated for 1 μM compound concentration after 24 h exposure (from 90.97% in CTRL to 86.79%). There was also an increase in the population of necrotic cells for 24 h exposure (from 8.03% in CTRL to 10.77% in 1 μM SAN) and apoptotic cells for 48 h treatment (from 1.08% for CTRL to 5.48% for 0.5 μM SAN) (Fig 2A, B). In turn, for RPMI-7951 cells after 24 h incubation with 1 μM SAN, a decrease in the percentage of viable cells was observed from 93.51% for CTRL to 80.9% and for 48 h from 92.1% to 33.57%. An increase in apoptotic cells population in comparison to untreated control was

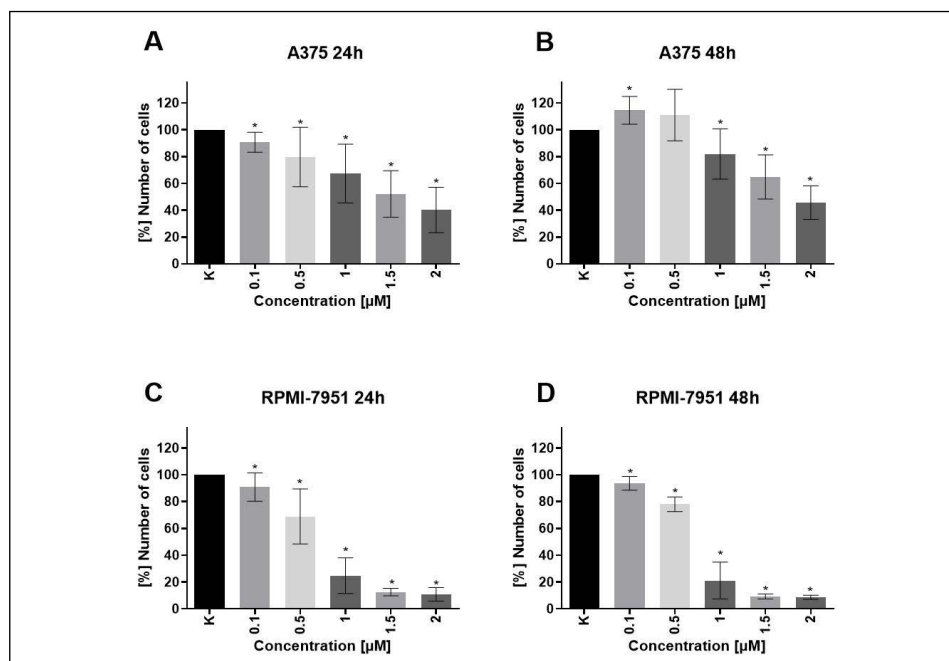


Figure 1. Analysis of sanguinarine (SAN) cytotoxicity on A375 (A, B) and RPMI-7951 (C, D). The effect of sanguinarine on the survival of human melanoma cells of the A375 and RPMI-7951 lines was assessed using the MTT test. The cells were treated with 0.1, 0.5, 1, 1.5, and 2 μM after 24 and 48 hours of exposure. *indicate statistically significant differences compared to control cells ($p < 0.05$; the non-parametric Wilcoxon test of two groups of variables)

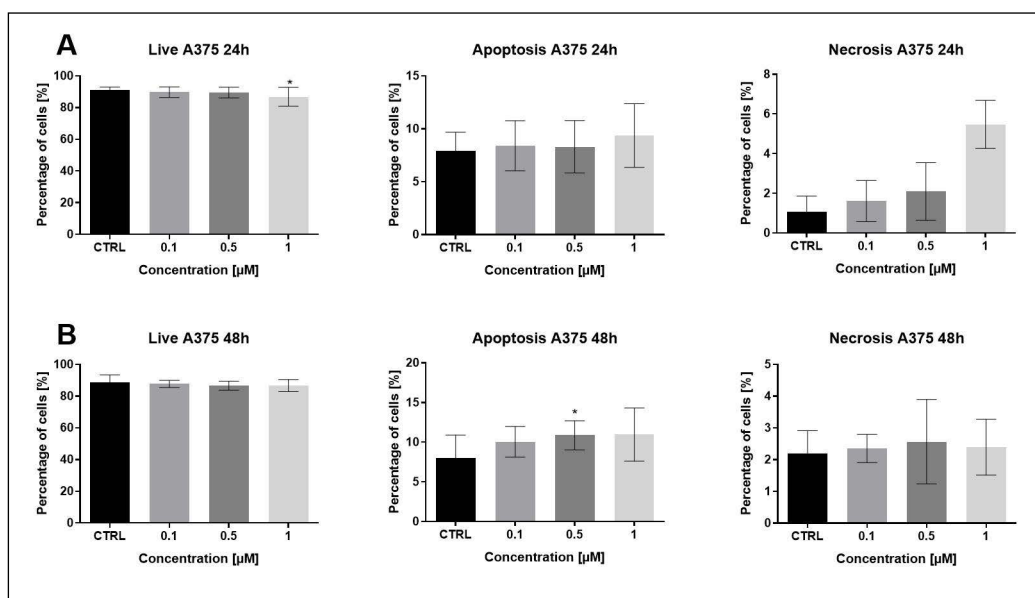


Figure 2. The effect of sanguinarine (SAN) on cell death of A375 cells. The cells were treated with 0.1, 0.5 and 1 mM SAN for 24 h (A) and 48 h (B). The cell death was analysed using a flow cytometer. The figure presents the percentage of live, apoptotic, and necrotic cells. *indicate statistically significant differences compared to control cells ($p < 0.05$; the non-parametric Kruskal-Wallis with Dunn's post hoc test)

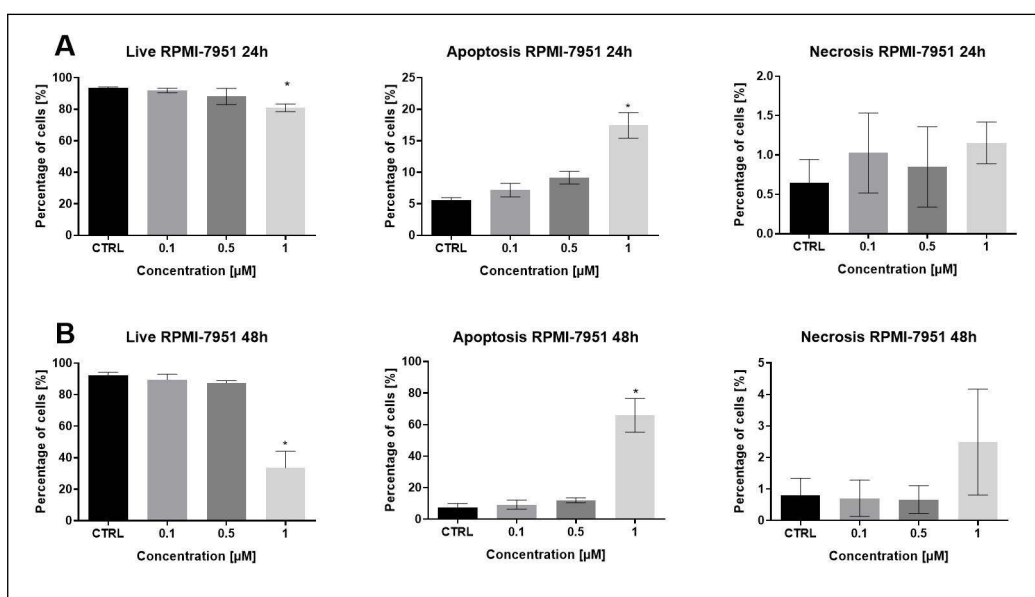


Figure 3. The effect of sanguinarine (SAN) on cell death of RPMI-7951 cells. The cells were treated with 0.1, 0.5 and 1 mM SAN for 24 h (A) and 48 h (B). The cell death was analysed using a flow cytometer. The figure presents the percentage of live, apoptotic, and necrotic cells. *indicate statistically significant differences compared to control cells ($p < 0.05$; the non-parametric Kruskal-Wallis with Dunn's post hoc test)

observed after exposure to 1 μ M SAN after 24 h (from 5.56 to 17.45%) and 48 h of exposure (from 7.53 to 65.84%) (Fig. 3A, B).

Cell cycle analysis showed significant differences for the G2/M phase at 1 μ M SAN (24h; from 35.18% in CTRL to 41.83%) and G0/G1 (48h) for A375 at 0.1 μ M

SAN and 1 μ M SAN (from 51.61% in CTRL to 61.37% and 62.19%, respectively) (Fig.4 A, B). In turn, incubation of the RPMI-7951 cells with SAN for 24 h resulted in changes in the G0/G1 phase for the applied dose of 0.1 and 0.5 μ M (from 48.72% in CTRL to 36.41% and 57.01%, respectively) and the S phase for 0.5 μ M SAN (from

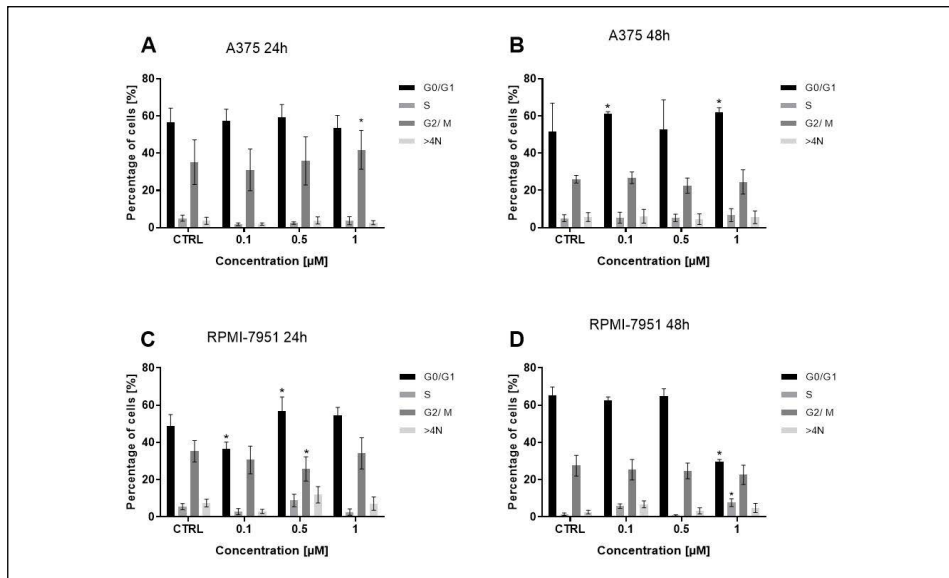


Figure 4. The effect of sanguinarine (SAN) on the cell cycle of A375 and RPMI-7951 cells. The cells were treated with 0.1, 0.5 and 1 mM SAN. The graphs presented A375 after 24 h treatment (A), 48 h (B) and RPMI-7951 after 24 h (C) and 48h (D). The cell cycle was analysed using a flow cytometer. *indicate statistically significant differences compared to control cells ($p < 0.05$; non-parametric 2way ANOVA with Dunnett's multiple comparisons test)

5.57% in CTRL to 25.78%). In turn, 1 μM dose of the alkaloid (48h) caused the greatest changes in the percentage of cells in the cell cycle phases (G0/G1 – from 65.35% in CTRL to 29.62%; S – from 1.45% in CTRL to 7.72%) (Fig. 4C, D).

Organization of main cytoskeletal proteins

In the case of F-actin labelling, a very slight long-term decrease in fluorescence intensity was observed in cells treated with increasing SAN doses (Fig. 5A–D). Control A375 cells for both incubation times with SAN (24 and 48 h) were characterized by a regular form of peripherally arranged actin filaments distributed within the entire cell. No significant changes in microfilaments were confirmed after treatment with 0.1 SAN for both 24 and 48 h. However, the entosis was noticed after exposure to 0.1 μM SAN. The cells of the A375 line are characterized by a well-developed network of intermediate filaments. Occasionally, a stronger signal of vimentin fluorescence was noted in different areas of the cytoplasm, with visible fibres in giant cells. However, in the case of both incubation times, no significant changes in vimentin fluorescence intensity of cells treated with the tested alkaloid were observed compared to control cells (Fig. 5E–H).

In the case of the second cell line, dose-dependent changes in the organization of F-actin were also observed. RPMI-7951 untreated cells showed a characteristic regular pattern of microfilaments. Single stress fibres were visible. With higher concentrations of SAN,

the number of stress fibres and point aggregates of this protein increased. In large cells, F-actin was dispersed in the cytoplasm. Moreover, the fluorescence intensity decreased slightly and destabilization of the actin cytoskeleton was evident in the shrunken cells. 1 μM SAN induced the highest decrease in F-actin intensity and its reorganization (after 24h and 48h). In addition, after 48h, microfilaments were more often concentrated mainly around the nucleus (Fig. 6A–D; M–P). After staining with vimentin, the highest fluorescence intensity was observed in RPMI-7951 control cells. The vimentin network was most prominent in cells with high cytoplasmic content. In addition, vimentin formed a distinct ring around the nucleus, which was particularly visible in large cells. A dose-dependent decrease in fluorescence intensity was also observed. In some partially shrunken cells, a concentration of vimentin was seen at the periphery of the cell membrane (Fig. 6E–H). Furthermore, with the use of increasing concentrations of SAN on RPMI-7951 and A375 cells, there was a decrease in the overall number of cells in comparison to the control, as well as a dose-dependent increase in intercellular spaces and impaired cell-cell contact, were observed (Fig. 5, 6).

Analysis of transwell migration assay

The migration potential was assessed using the transwell migration assay. In A375 cells both incubation times induced a reduction in the number of cells with high migratory abilities. Statistically significant changes were noted for 0.5 and 1 μM doses after 24 h exposure,

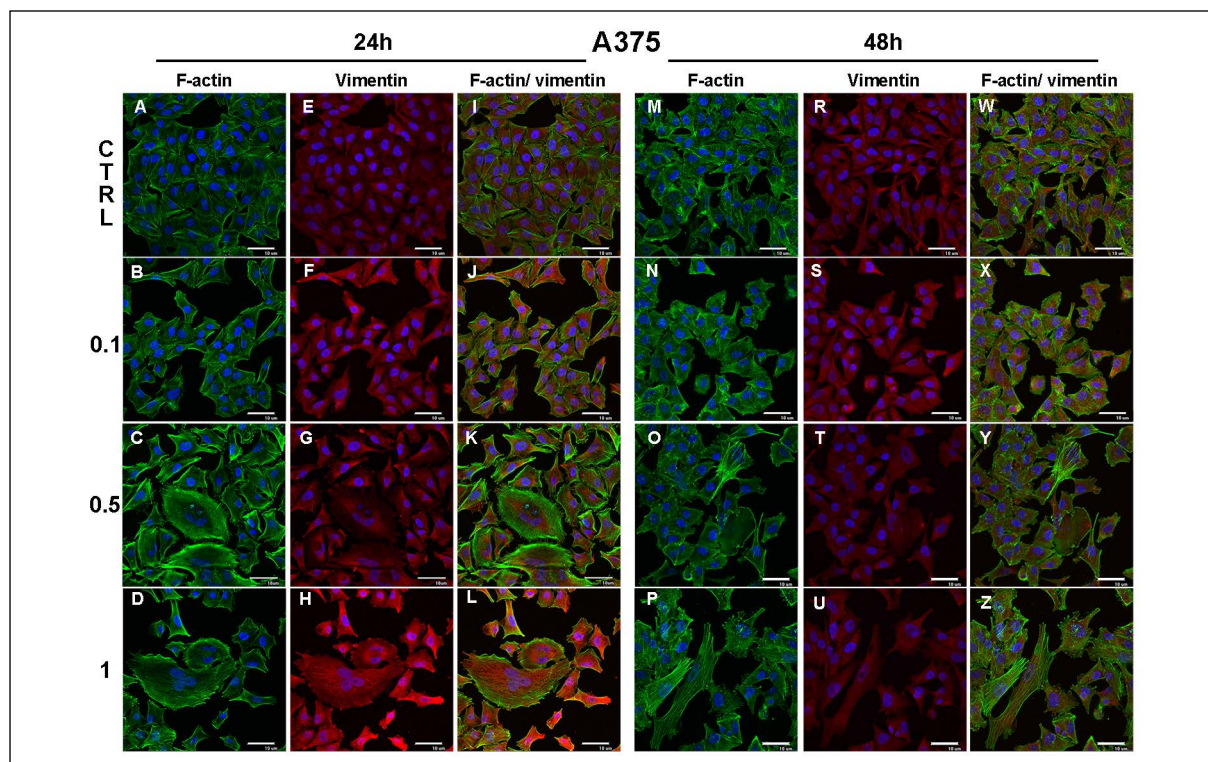


Figure 5. The effect of sanguinarine (SAN) on the F-actin and vimentin organization of A375 cells. The cells were treated with 0.1, 0.5 and 1 mM SAN for 24 h (A–L) and 48 h (M–Z). Immunofluorescent labelling of F-actin (green), vimentin (red), and nuclei (blue), Bar = 10 μ m

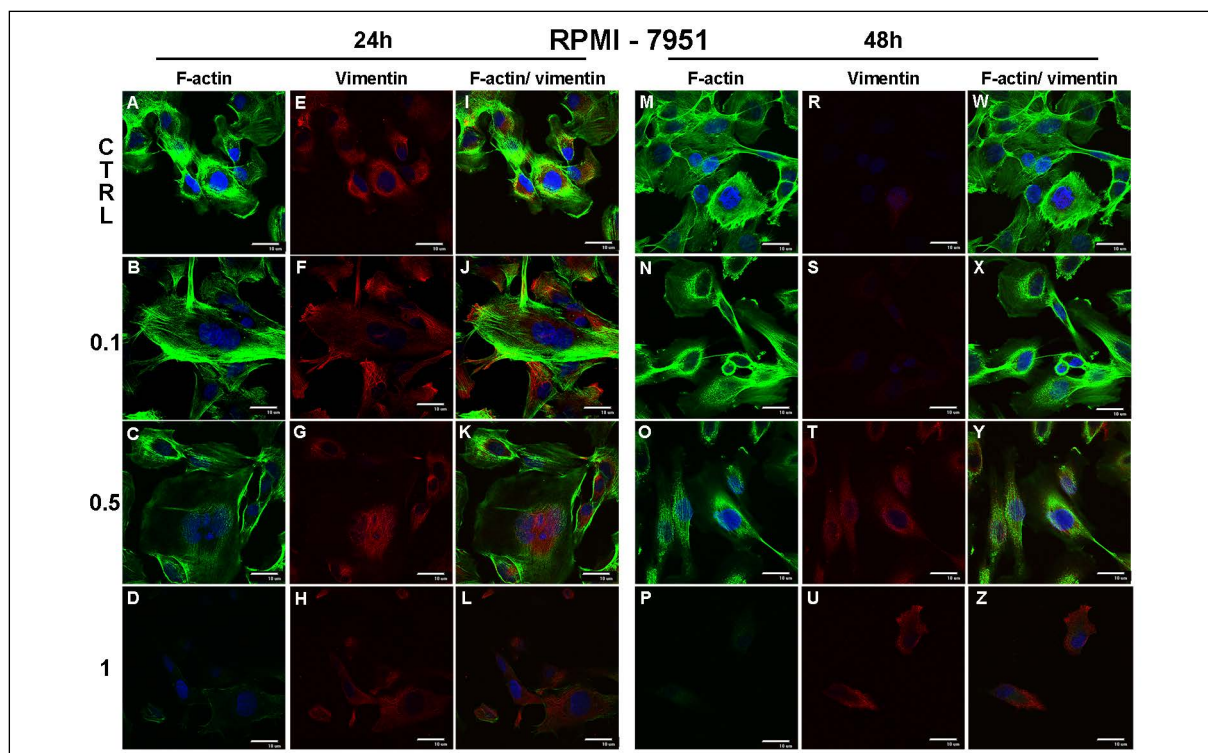


Figure 6. The effect of sanguinarine (SAN) on the F-actin and vimentin organization of RPMI-7951 cells. The cells were treated with 0.1, 0.5 and 1 mM SAN for 24 h (A–L) and 48 h (M–Z). Immunofluorescent labelling of F-actin (green), vimentin (red), and nuclei (blue), Bar = 10 μ m

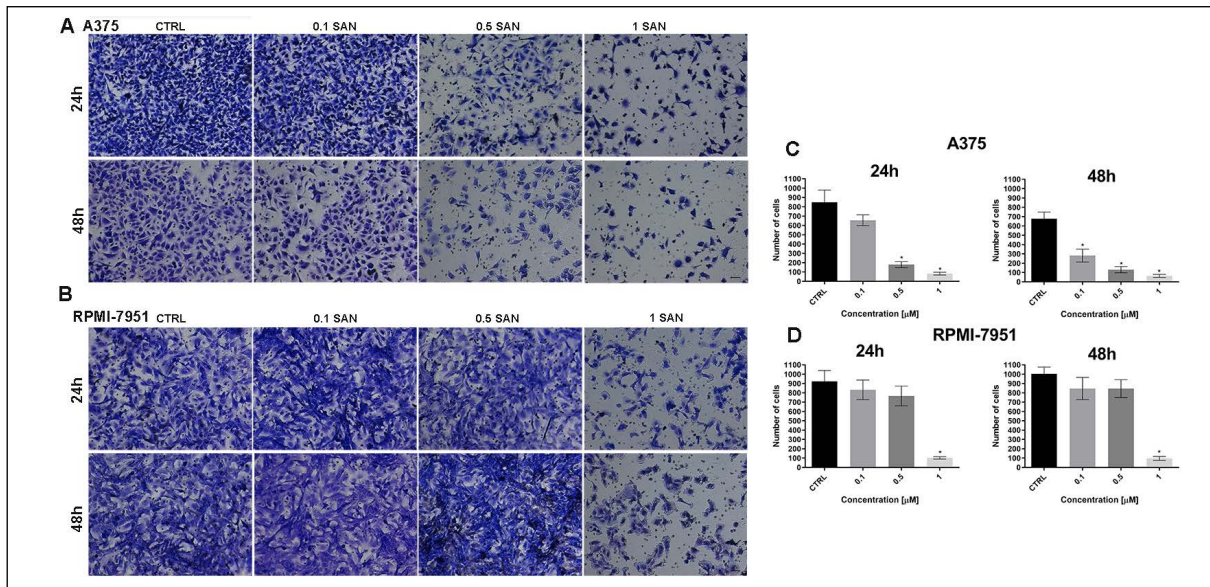


Figure 7. The effect of sanguinarine (SAN) on the migration potential of A375 and RPMI-7951 cells. Transwell migration assay. The representative images of the results obtained in Transwell migration assay, Bar = 50 μm (A, B). The average number of A375 (C) and RPMI-7951 (D) cells with high migratory potential in comparison to control cells. *indicate statistically significant differences in comparison to control cells ($p < 0.05$; Kruskal-Wallis with Dunn's post hoc test)

and for all concentrations after 48 h incubation. At the highest dose, the number of cells that crossed the insert membrane was 82.6 (24 h) and 63.4 (48 h) (Fig. 7A, C). In the case of RPMI-7951, only the highest dose of SAN resulted in a statistically significant reduction in the migration potential of cells. 102.4 and 96.5 cells were observed after 24 h and 48 h incubation, respectively (Fig. 7B, D).

Discussion

Nowadays, the most common oncological diseases include breast, lung, colorectal, liver, and prostate cancer. Melanoma is the most malignant cancer occurring in the skin. The number of melanoma cases is increasing. Despite highly developed medicine, melanoma still belongs to the group of cancers that are most resistant to standard oncological treatment [11]. For this reason, phytochemicals or their derivatives that could be officially implemented in anti-cancer therapies are sought. The possibility of creating such drugs is demonstrated by paclitaxel and vincristine, which are compounds of plant origin used in anticancer therapy [12]. These include sanguinarine, which is representative of plant alkaloids. It has been proven that it has antibacterial and anti-inflammatory properties and what is important in the context of oncological therapy — the anti-cancer effect.

There are few literature reports on the effect of SAN on the A375 and RPMI-7951 cell lines. Thus, the presented study aimed to evaluate how the alkaloid

impacts the basic life processes of two melanoma cell lines A375 and RPMI-7951.

The results of the MTT assay in A375 and RPMI-7951 melanoma cells showed a dose-dependent sensitivity to the alkaloid after 24 and 48 hours of exposure. This effect is in line with the research of Hammerová et al. (2011), who also studied the impact of SAN on the A375 cell line. The cells were treated with SAN in the concentration range of 0.1–3 $\mu\text{g}/\text{ml}$. The authors demonstrated that the metabolic activity of cells decreased with the increase in the concentration of the compound [13]. Similar results were obtained by Cojocaru et al. (2006), who assessed the cytotoxic effect of SAN on cells of the C32 amelanotic melanoma cell line. The doses of alkaloid used were 0.5, 1, and 2 μM and generated a dose-dependent decrease in cell survival [14]. In turn, Tuzimski et al. (2021) tested SAN on three types of melanoma cells – A375, G361, and SKMEL3. They reported that the IC₅₀ for the alkaloid was estimated to be less than 0.55 $\mu\text{g}/\text{mL}$ for selected lines, and the A375 cells were the most sensitive [15].

The results obtained in this study do not allow us to draw a clear conclusion that it is apoptosis or necrosis that causes the death of the A375 cells treated with selected doses of SAN. However, cells presenting other types of cell death such as entosis and possibly mitotic catastrophe have been noted. Nevertheless, the lack of literature data does not allow us to state that alkaloid directly induces these processes. In the case of the second line, RPMI-7951, the highest concentration of SAN (1 μM) induced a very high percentage of apoptotic

cells, especially after 48 h of exposure. Studies by Hammerová et al. (2011) on the A375 cell line showed that treatment of cells with SAN in the doses of 0.1–3 $\mu\text{g/ml}$ results in a decrease in the level of the anti-apoptotic protein Bcl-xL. Moreover, SAN at 0.1 $\mu\text{g/ml}$, 0.5 $\mu\text{g/ml}$, and 1 $\mu\text{g/ml}$ concentrations reduces the level of XIAP protein, which is an inhibitor of apoptosis [13]. On the other hand, studies by Kemeny-Beke et al. (2006) on human primary OCM-1 lines have shown that SAN (1.4 and 8 $\mu\text{g/ml}$) causes cell death by apoptosis and necrosis [16]. In turn, Serafim et al. (2008), who tested SAN on K1735-M2 mouse melanoma cells, reported that the alkaloid induces apoptosis via mitochondrial changes and DNA damage [17].

In A375 cells, the cell cycle analysis showed the arrest in G2/M (24 h treatment) or G0/G1 (48 h treatment) phase, especially for 1 μM SAN. In turn, RPMI-7951, as in the case of apoptosis, turned out to be more sensitive to the action of the alkaloid. For the highest concentration of SAN, the G0/G1 fraction was significantly reduced. Studies conducted on the effect of SAN (1.25–20 μM) on a mouse model of melanoma — the K1735-M2 cell line, also indicate the anti-proliferative action and the cell cycle arrest in the subG1 phase [17]. The anti-cancer potential of sanguinarine manifested by the ability to block the cell cycle has also been confirmed in studies on other types of cancer. Adhami et al. (2004) showed that in prostate cancer cells of the LNCaP and DU145 cell lines, the 0.2–2 $\mu\text{mol/L}$ doses of sanguinarine, cause a dose-dependent decrease in the expression of cyclins D1, D2, and E, as well as CDK 2, 4, and 6. The authors claim that this causes a blockade of the G1-S transition in the cell cycle, which results in sanguinarine-induced arrest of the G0-G1 phase and consequently leads to cell death [18]. In turn, Zhang et al. (2017) applied sanguinarine at concentrations of 5, 10, and 30 $\mu\text{mol/L}$ in gastric cancer cells. The researchers observed that the tested compound inhibits cell viability and induces cell apoptosis and S-phase arrest [19].

Microscopic analysis of A375 and RPMI-7951 cells treated with SAN provided information about the effect of the test compound on the morphology and the main cytoskeletal proteins of melanoma cells. The applied compound caused a dose-dependent decrease in the number of cells and impaired intercellular interactions. In the case of A375, shrunken cells with condensed cytoplasm, entosis, and cells with large nuclei or micronuclei with mitotic catastrophe characteristics were noted. In turn, morphological changes in RPMI-7951 were also manifested by shrunken cytoplasm and chromatin condensation in nuclei. A small population of oval and shrunken cells after treatment with 1 μM SAN was observed, which may be due to the intense cell death-inducing effect. Kemeny-Beke et al. (2006), using human primary cells of the OCM-1 line, reported

that the concentration of 8 $\mu\text{g/ml}$ of sanguinarine induces the formation of swollen and enlarged cells, as well as shrunken cells with apoptotic morphology [16]. Similar results were obtained by Cojocar et al. (2016) on C32 amelanotic melanoma cell line [14]. In turn, Serafim et al. (2008) showed that 8 μM initiates rounding of K1735-M2 mouse melanoma cells and changes in the cell nucleus with clearly noticeable chromatin condensation [17]. The effect of the alkaloid on cell morphology can also be observed in other cancers. Lee et al. proved that SAN in the doses of 0.5, 1, and 2 μM causes a dose-dependent decrease in the survival of HT-29 colorectal cancer cells. The authors indicate the presence of rounded and shrunken cells, as well as cells with a degraded and fragmented cell nucleus [20].

There are no literature data on the effect of SAN on the elements of the cytoskeleton of A375 and RPMI-7951 cells. For both melanoma cell lines used in the present study, depolymerization of F-actin fibres and the presence of stress fibres were observed. Cells, where F-actin is present in the form of small aggregates and short polymers, were also noted. A dose-dependent decrease in vimentin fluorescence intensity was observed with RPMI-7951. Despite the lack of results referring explicitly to the vimentin network of A375 cells in this work, literature data indicate the influence of SAN on this protein of intermediate filaments. Similar observations regarding the effect of SAN on the cellular cytoskeleton have been reported in experiments on other cancer cell lines. Studies on liver cancer cells evaluating the anti-proliferative and EMT-reversing effects of the alkaloid have shown that the tested compound inhibits the expression of vimentin, which is a marker of the epithelial-mesenchymal transition [21].

The last stage of the research was the assessment of the migration potential of the cells. In both cases, the greatest reduction in migratory abilities was observed for the highest dose of SAN (1 μM), both for 24 and 48 h incubation periods. In the authors' opinion, fewer cells that crossed the insert in the transwell migration assay correlate with reduced fluorescence intensity of the F-actin network, changes in cell shape to more oval, and widening of intercellular spaces. Unfortunately, there are no literature reports in the context of the influence of SAN on melanoma cell migration. However, numerous reports of sanguinarine's anti-migration properties refer to other cell lines, including breast, lung, and colorectal [22, 23]. Scientists explain this effect based on changes in the wnt/ β -catenin pathway, reduction in the level of metalloproteins and EMT markers (N-cadherin, vimentin, and Snail), or VEGF inhibition [23, 24].

Due to the high malignancy of melanoma, the frequency of its occurrence, and resistance to standard oncological treatment, new therapeutic strategies are of great importance. This study's results on the effect

of sanguinarine on human melanoma cells of the A375 and RPMI-7951 cell lines confirm the anti-cancer properties of the alkaloid (cytotoxicity, anti-migratory, and pro-apoptotic action). In addition, it was observed that RPMI-7951 cells were more sensitive to SAN than A375, which was manifested by a higher percentage of apoptotic cells at both incubation times. To the authors' knowledge, it is the first report on the compound's effect on RPMI-7951 lines. However, further research is needed to verify its effectiveness and safety.

Acknowledgements: *This study was supported by a research task within the framework of the Department of Histology and Embryology (Nicolaus Copernicus University in Torun, Faculty of Medicine, Collegium Medicum in Bydgoszcz).*

Conflict of interests: *None.*

Funding: *None.*

References

- Slominski A, Wortsman J, Carlson AJ, et al. Malignant melanoma. Arch Pathol Lab Med. 2001; 125(10): 1295–1306, doi: [10.5858/2001-125-1295-MM](https://doi.org/10.5858/2001-125-1295-MM), indexed in Pubmed: [11570904](https://pubmed.ncbi.nlm.nih.gov/11570904/).
- Rastrelli M, Tropea S, Rossi CR, et al. Melanoma: epidemiology, risk factors, pathogenesis, diagnosis and classification. In Vivo. 2014; 28(6): 1005–1011, indexed in Pubmed: [25398793](https://pubmed.ncbi.nlm.nih.gov/25398793/).
- Namikawa K, Yamazaki N. Targeted Therapy and Immunotherapy for Melanoma in Japan. Curr Treat Options Oncol. 2019; 20(1): 7, doi: [10.1007/s11864-019-0607-8](https://doi.org/10.1007/s11864-019-0607-8), indexed in Pubmed: [30675668](https://pubmed.ncbi.nlm.nih.gov/30675668/).
- Burgeiro A, Bento AC, Gajate C, et al. Rapid human melanoma cell death induced by sanguinarine through oxidative stress. Eur J Pharmacol. 2013; 705(1-3): 109–118, doi: [10.1016/j.ejphar.2013.02.035](https://doi.org/10.1016/j.ejphar.2013.02.035), indexed in Pubmed: [23499690](https://pubmed.ncbi.nlm.nih.gov/23499690/).
- Achkar IW, Mraiche F, Mohammad RM, et al. Anticancer potential of sanguinarine for various human malignancies. Future Med Chem. 2017; 9(9): 933–950, doi: [10.4155/fmc-2017-0041](https://doi.org/10.4155/fmc-2017-0041), indexed in Pubmed: [28636454](https://pubmed.ncbi.nlm.nih.gov/28636454/).
- Mackraj I, Govender T, Gathiram P. Sanguinarine. Cardiovasc Ther. 2008; 26(1): 75–83, doi: [10.1111/j.1527-3466.2007.00037.x](https://doi.org/10.1111/j.1527-3466.2007.00037.x), indexed in Pubmed: [18466423](https://pubmed.ncbi.nlm.nih.gov/18466423/).
- Prabhu KS, Bhat AA, Siveen KS, et al. Sanguinarine mediated apoptosis in Non-Small Cell Lung Cancer via generation of reactive oxygen species and suppression of JAK/STAT pathway. Biomed Pharmacother. 2021; 144: 112358, doi: [10.1016/j.biopha.2021.112358](https://doi.org/10.1016/j.biopha.2021.112358), indexed in Pubmed: [34794241](https://pubmed.ncbi.nlm.nih.gov/34794241/).
- Hałas-Wiśniewska M, Zielińska W, Izdebska M, et al. The Synergistic Effect of Piperlongumine and Sanguinarine on the Non-Small Lung Cancer. Molecules. 2020; 25(13), doi: [10.3390/molecules25133045](https://doi.org/10.3390/molecules25133045), indexed in Pubmed: [32635287](https://pubmed.ncbi.nlm.nih.gov/32635287/).
- Basu P, Kumar GS. Sanguinarine and Its Role in Chronic Diseases. Adv Exp Med Biol. 2016; 928: 155–172, doi: [10.1007/978-3-319-41334-1_7](https://doi.org/10.1007/978-3-319-41334-1_7), indexed in Pubmed: [27671816](https://pubmed.ncbi.nlm.nih.gov/27671816/).
- Rosen J, Landriscina A, Adler BL, et al. Characterization and assessment of nanoencapsulated sanguinarine chloride as a potential treatment for melanoma. J Drugs Dermatol. 2015; 14(5): 453–458, indexed in Pubmed: [25942662](https://pubmed.ncbi.nlm.nih.gov/25942662/).
- Olbryt M. [Role of tumor microenvironment in the formation and progression of skin melanoma]. Postepy Hig Med Dosw (Online). 2013; 67: 413–432, doi: [10.5604/17322693.1049286](https://doi.org/10.5604/17322693.1049286), indexed in Pubmed: [23756376](https://pubmed.ncbi.nlm.nih.gov/23756376/).
- Xiao Xu, Hou X, Shi W, et al. Oxymatrine inhibits proliferation and apoptosis of human breast cancer cells through the regulation of miRNA-140-5P. Am J Transl Res. 2021; 13(12): 13674–13682, indexed in Pubmed: [35035706](https://pubmed.ncbi.nlm.nih.gov/35035706/).
- Hammerová J, Uldrijan S, Táborská E, et al. Benzo[c]phenanthridine alkaloids exhibit strong anti-proliferative activity in malignant melanoma cells regardless of their p53 status. J Dermatol Sci. 2011; 62(1): 22–35, doi: [10.1016/j.jdermsci.2011.01.006](https://doi.org/10.1016/j.jdermsci.2011.01.006), indexed in Pubmed: [21324654](https://pubmed.ncbi.nlm.nih.gov/21324654/).
- Cojocarau S, Stan M, Anton M, et al. The cytotoxic activity of sanguinarine in C32 human amelanotic melanoma cells. Turkish Journal of Biology. 2016; 40: 130–138, doi: [10.3906/biy-1501-52](https://doi.org/10.3906/biy-1501-52).
- Tuzimski T, Petruczynik A, Plech T, et al. Determination of Cytotoxic Activity of Extracts against Human Melanoma Cells and Comparison of Their Cytotoxicity with Cytotoxicity of Some Anticancer Drugs. Molecules. 2021; 26(6), doi: [10.3390/molecules26061738](https://doi.org/10.3390/molecules26061738), indexed in Pubmed: [33804614](https://pubmed.ncbi.nlm.nih.gov/33804614/).
- Kemény-Beke A, Aradi J, Damjanovich J, et al. Apoptotic response of uveal melanoma cells upon treatment with chelidonine, sanguinarine and chelerythrine. Cancer Lett. 2006; 237(1): 67–75, doi: [10.1016/j.canlet.2005.05.037](https://doi.org/10.1016/j.canlet.2005.05.037), indexed in Pubmed: [16019128](https://pubmed.ncbi.nlm.nih.gov/16019128/).
- Serafim TL, Matos JAC, Sardão VA, et al. Sanguinarine cytotoxicity on mouse melanoma K1735-M2 cells--nuclear vs. mitochondrial effects. Biochem Pharmacol. 2008; 76(11): 1459–1475, doi: [10.1016/j.bcp.2008.07.013](https://doi.org/10.1016/j.bcp.2008.07.013), indexed in Pubmed: [18692024](https://pubmed.ncbi.nlm.nih.gov/18692024/).
- Adhami VM, Aziz MH, Reagan-Shaw SR, et al. Sanguinarine causes cell cycle blockade and apoptosis of human prostate carcinoma cells via modulation of cyclin kinase inhibitor-cyclin-dependent kinase machinery. Mol Cancer Ther. 2004; 3(8): 933–940, indexed in Pubmed: [15299076](https://pubmed.ncbi.nlm.nih.gov/15299076/).
- Zhang R, Wang Ge, Zhang PF, et al. Sanguinarine inhibits growth and invasion of gastric cancer cells via regulation of the DUSP4/ERK pathway. J Cell Mol Med. 2017; 21(6): 1117–1127, doi: [10.1111/jcmm.13043](https://doi.org/10.1111/jcmm.13043), indexed in Pubmed: [27957827](https://pubmed.ncbi.nlm.nih.gov/27957827/).
- Lee JS, Jung WK, Jeong MHO, et al. Sanguinarine induces apoptosis of HT-29 human colon cancer cells via the regulation of Bax/Bcl-2 ratio and caspase-9-dependent pathway. Int J Toxicol. 2012; 31(1): 70–77, doi: [10.1177/1091581811423845](https://doi.org/10.1177/1091581811423845), indexed in Pubmed: [22215411](https://pubmed.ncbi.nlm.nih.gov/22215411/).
- Su Qi, Fan M, Wang J, et al. Sanguinarine inhibits epithelial-mesenchymal transition via targeting HIF-1 α /TGF- β feed-forward loop in hepatocellular carcinoma. Cell Death Dis. 2019; 10(12): 939, doi: [10.1038/s41419-019-2173-1](https://doi.org/10.1038/s41419-019-2173-1), indexed in Pubmed: [31819036](https://pubmed.ncbi.nlm.nih.gov/31819036/).
- Wang X, Decker CC, Zechner L, et al. In vitro wound healing of tumor cells: inhibition of cell migration by selected cytotoxic alkaloids. BMC Pharmacol Toxicol. 2019; 20(1): 4, doi: [10.1186/s40360-018-0284-4](https://doi.org/10.1186/s40360-018-0284-4), indexed in Pubmed: [30626448](https://pubmed.ncbi.nlm.nih.gov/30626448/).
- Zhu M, Gong Z, Wu Q, et al. Sanguinarine suppresses migration and metastasis in colorectal carcinoma associated with the inversion of EMT through the Wnt/ β -catenin signaling. Clin Transl Med. 2020; 10(1): 1–12, doi: [10.1002/ctm2.1](https://doi.org/10.1002/ctm2.1), indexed in Pubmed: [32508048](https://pubmed.ncbi.nlm.nih.gov/32508048/).
- Xu JY, Meng QH, Chong Yu, et al. Sanguinarine is a novel VEGF inhibitor involved in the suppression of angiogenesis and cell migration. Mol Clin Oncol. 2013; 1(2): 331–336, doi: [10.3892/mco.2012.41](https://doi.org/10.3892/mco.2012.41), indexed in Pubmed: [24649171](https://pubmed.ncbi.nlm.nih.gov/24649171/).